Mariam K. Glob [1]
Khalidah H. Al-Mayalee [1]
Saleem A. Hussain [2]

[1] *Department of Physics, College of Education for Girls, University of Kufa, Al-Najaf , IRAQ*
[2] *Department of Physics, College of Education, University of Al-Qadisiyah, Al-Diwaniyah, IRAQ*

Characterization of Titanium Dioxide Nanoparticles Synthesized By Microwave Method

In this study, titanium dioxide (TiO_2) nanoparticles were fast and cheaply synthesized using microwave methods. Titanium isopropoxide ($Ti[OCH(CH_3)_2]_4$) was used as a precursor and deionized water (DW) was used as the solvent and reduction agent for sub-micrometer particle production after 5 minutes annealing at 400 °C for 1 hour using a 1200W commercial microwave instrument. The structural characterization tests showed that the anatase phase is the dominant in the prepared TiO_2 nanoparticles. Large TiO_2 surface area of 72.727 to 108.28 m^2/g was confirmed. Spherical and irregular particles with uniform distribution and average diameters of 52.707, 65.602, and 82.095 nm were shown. Highly-pure TiO_2 nanoparticles with strong Ti and O peaks were produced.

Keywords: Titanium dioxide; Nanoparticles; Titanium isopropoxide; Microwave method
Received: 18 October 2023; **Revised:** 13 November; **Accepted:** 20 November 2023

1. Introduction

Titanium dioxide (TiO_2), also known as titania, is a white inorganic solid that insoluble in water, chemically inert, and nonflammable. It is used extensively in the manufacture of catalyst supports, solar cells, and various consumer goods, such as cosmetics, coatings, paints, ceramics, and textiles [1-3]. TiO_2, a transition metal oxide, is typically derived from leucoxene ores or limonite because it does not exist naturally [4]. Titanium, the ninth most abundant element, is found in compounds in rocks and mineral sand. Nanostructured TiO_2, owing to its size-dependent characteristics, offers a large surface area for adsorption and catalysis [5]. TiO_2 has three primary phase structures: brookite, anatase, and rutile, with anatase demonstrating superior photoactivity [6]. Although rutile is thermodynamically stable, anatase outperforms it in photocatalytic reactions owing to its lower electron-hole recombination rate. The synthesis of pure anatase photocatalysts remains a challenge [7-10].

The study aims to synthesize TiO_2 nanoparticles of unique properties by microwave method using titanium isopropoxide ($Ti[OCH(CH_3)2]_4$) and deionized water (DW). The structural characteristics of the synthesized samples were determined.

2. Experimental Part

The synthesis of TiO_2 powder was conducted utilizing a microwave-assisted technique using a Sharp-38L microwave oven operating at a frequency of 2.45 GHz. The experimental methodology involved the utilization of titanium (IV) isopropoxide ($Ti[OCH(CH_3)2]_4$) (TTIP) as the precursor, deionized water (DW) as the solvent, and reducing agents for the synthesis of sub micrometer particles. In the method, a volume of 10 ml of TTIP was incrementally introduced into a glass jar containing 100 ml of DW. This was accomplished by utilizing a magnetic stirrer operating at a speed of 600 r.p.m for 10 minutes. The synthesis was carried out for 5 minutes with power levels set at 40%, 60%, and 100% of the maximum output power (1200 W). The solution underwent a transformation, transitioning from a transparent state to a milky white appearance, which serves as an indication of the formation of TiO_2 nanoparticles (Fig. 1a).

(a) (b) (c)

Fig. (1) Steps of synthesis process (a) the milky white solution after the titration process, (b) the collected powder after washing with ethanol and de-ionized water, and (c) the final product after annealing at 400°C for 1 h

The resultant precipitate was gathered, subjected to rinsing with deionized water (DW) and 100% ethanol, and thereafter subjected to centrifugation at a speed of 4500 r.p.m for 5 minutes (Fig. 1b). The powder was subjected to a drying process in an oven set at a temperature of 60°C for one hour. Subsequently, it was stored in the oven overnight.

Following that, the powder underwent calcination at a temperature of 400°C within a furnace (ELF 11/14B) under atmospheric conditions for one hour (as depicted in Fig. 1c).

3. Results and Discussion

Figure (2) shows the x-ray diffraction (XRD) patterns of the synthesized TiO_2 nanoparticles. Based on these patterns, the peaks indicate the formation of nanomaterials with high crystallization. It can be deduced that the synthesized TiO_2 nanoparticles exist in the anatase phase (JCPDS card no. 21-1272). The diffraction peaks of the prepared samples reveal a sharp domain (101) peak at approximately $2\theta=25.33°$, ascribed to the tetragonal structure of the TiO_2 phase with anatase lattice constants $a=b=0.37852$ nm, $c=0.65139$ nm, and angles $\alpha=\beta=\gamma=90°$. The XRD patterns also showed that there were no peaks of other materials, indicating that the samples were prepared with a high degree of purity. Furthermore, through the examination of Fig. (2) and a thorough analysis of the XRD results, it is evident that the data acquired for three different power levels (40%, 60%, and 100%) of the microwave radiation exhibit a significant level of convergence and concurrence with the values of 2θ and inter-planar distance (d) as indicated in the standard JCPDS card. Additionally, the positions of the peaks for all three cases align, with a noticeable enhancement in the intensity of the peaks observed at a microwave power of 100%. The average crystallite size of the synthesized TiO_2 nanoparticles was determined by broadening the anatase TiO_2 peaks at different 2θ values in the model using the Debye–Scherrer formula [11].

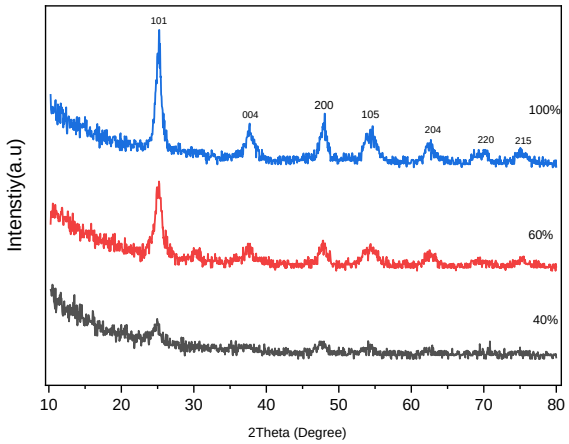

Fig. (2) XRD pattern of the synthesized TiO_2 nanoparticles with different microwave powers

In table (1), the results shows that the average crystallite size of the prepared samples are 3.73 to 8.46 nm. The uniform microwave heating mechanism results in homogeneous heating of the TiO_2 material, which leads to the formation of an anatase phase within a very short time [12,13].

Table (1) The average crystallite sizes of the synthesized TiO_2 nanoparticles

Microwave power	Average crystallite size (D) (nm)
40%	3.73
60%	5.98
100%	8.46

Figures (3), (4) and (5) show that the results of the typical nitrogen (N_2) adsorption and desorption isotherms of TiO_2 nanoparticles synthesized with 40%, 60%, and 100% of microwave power, respectively. The irregular distribution of pore sizes in the prepared nanoparticles resulted in hysteresis loops between the adsorption and desorption curves. The purpose of using inert nitrogen gas in this test is to remove any absorbent molecules from the material. Hysteresis loops between the adsorption and desorption curves are fundamental and important in determining some details of the nanostructures of the prepared samples.

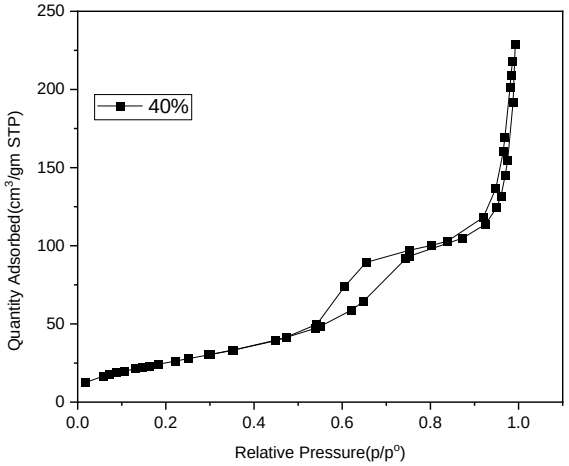

Fig. (3) The N_2 adsorption-desorption of TiO_2 nanoparticles with 40% microwave power

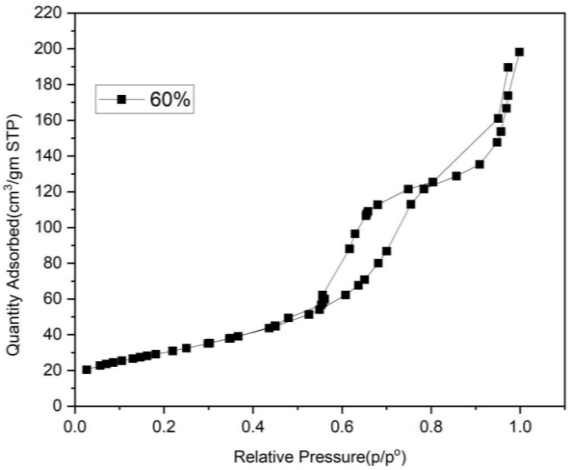

Fig. (4) The N_2 adsorption-desorption of TiO_2 nanoparticles synthesized with 60% microwave power

The presence of the aforementioned hysteresis loop indicates an accurate description of the pores in the nanomaterial based on the size and area of the loop. The isotherm linear plot shows the change in the quantity adsorbed with respect to p/p_0. A gradual

change in the adsorption desorption branch under a substantial pressure range (p/p_0) is shown in the isotherm of the synthesized samples, which indicates the presence of a porous material.

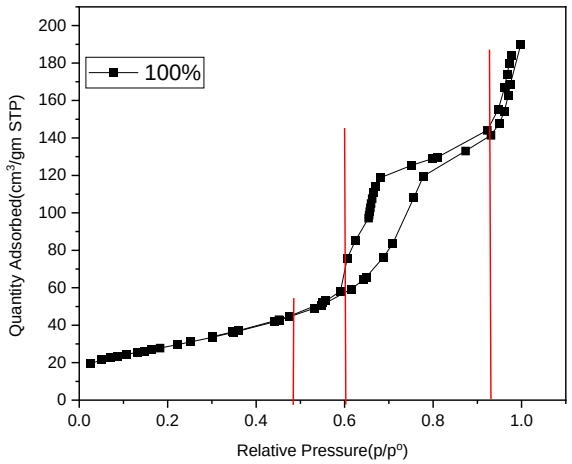

Fig. (5) The N_2 adsorption-desorption of TiO_2 nanoparticles synthesized with 100% microwave power

In the samples prepared at 40%, 60%, and 100% of microwave power for 5 min, four regions appeared in the isotherm linear plot. As shown in Fig. (6), the isotherm can be divided into four regions: the first region is at a relative pressure (p/p_0) below 0.5, and the isotherm shows a gradual increase in adsorption, which indicates that the samples have micropores. In the second region, the relative pressure was between 0.5 and 0.6, and the isotherm showed weak hysteresis loops; the samples contained mesopores [14,15]. In the third region, the isotherm reveals a distinct capillary concentration when the relative pressure is between 0.6 and 0.92. Finally, in the fourth region, with the highest relative pressure above 0.92, a small hysteresis loop can be observed, indicating the existence of larger mesopores [16].

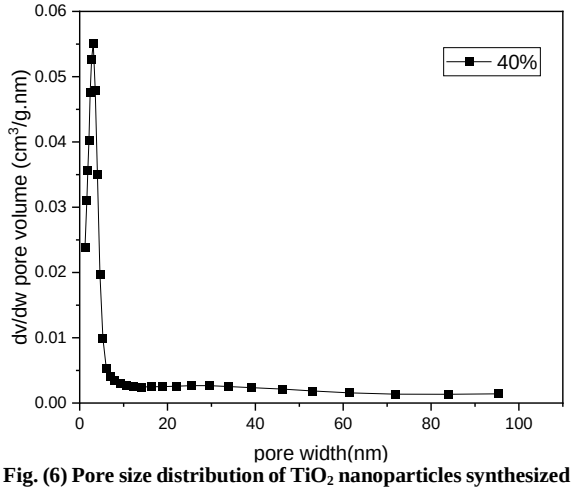

Fig. (6) Pore size distribution of TiO_2 nanoparticles synthesized with 40% microwave power

Through using Barret-Joyner-Halenda (BJH) method, the pore size of the distribution pattern was evaluated from the N_2 isotherm desorption branch [17], as shown in figures (6) (7) and (8). The results show that the average pore size of the prepared samples synthesized by the microwave method (40%, 60%, and 100%) was about 3.52, 3.55, and 4.02 nm, respectively, and the average pore volume was about 0.062, 0.057, 0.073 cm^3/g, respectively. This agrees with [18].

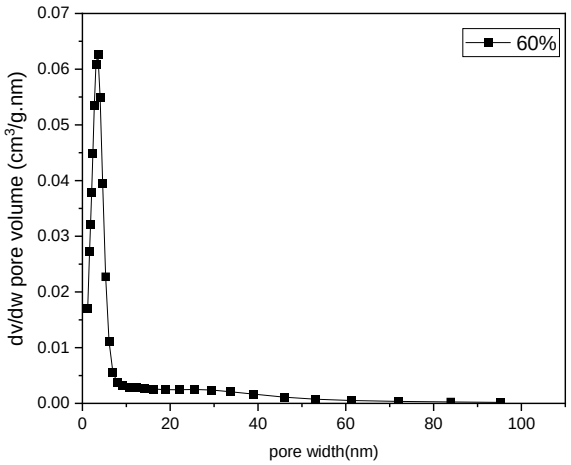

Fig. (7) Pore size distribution of TiO_2 nanoparticles synthesized with 60% microwave power

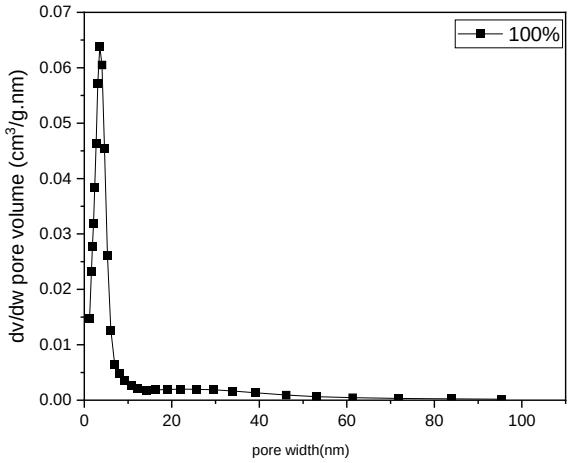

Fig. (8) Pore size distribution of TiO_2 nanoparticles synthesized with 100% microwave power

Figures (9) (10) and (11) show the surface morphology of the prepared samples as determined by the field-emission scanning electron microscopy (FE-SEM). For the samples synthesized with 40%, 60%, and 100% of the microwave power, the FE-SEM images show the spherical clusters distributed in different regions with an average size of 52.707, 65.602 and 82.095 nm for the samples synthesized with 40%, 60%, and 100% of microwave power, respectively, as shown in table (2). A closer view of the FE-SEM images showed a rough surface and high pore size, which resulted in high specific surface areas for these samples. This observation was in agreement with the BET results. Generally, it was concluded that there is a proportional relationship between microwave power and particle size.

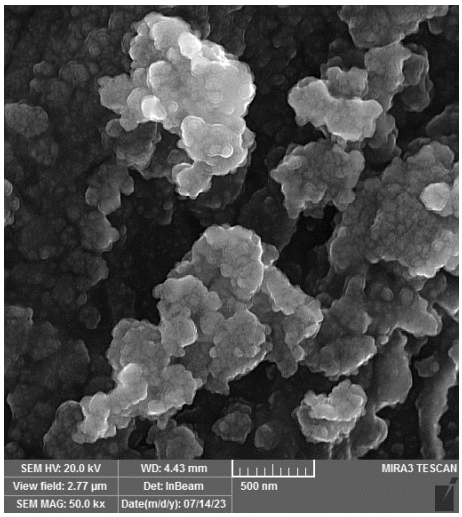

Fig. (9) FE-SEM of TiO_2 nanoparticles synthesized with 40% microwave power

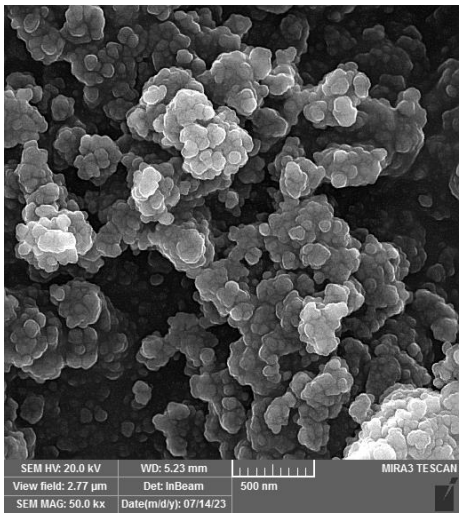

Fig. (10) FE-SEM of TiO_2 nanoparticles synthesized with 60% microwave power

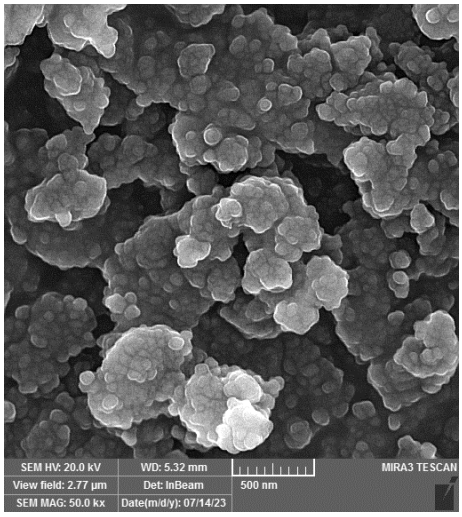

Fig. (11) FE-SEM of TiO_2 nanoparticles synthesized with 100% microwave power

Table (2) The average lengths, diameters, and aspect ratio of TiO_2 nanoparticles prepared with 40%,60%,100% microwave power

Microwave power	Average length (nm)	Average diameter (nm)	Aspect ratio (length/diameter)
40%	630	122	14.64
60%	1800	150	17.94
100%	2600	210	21.2

Figures (12) (13) and (14) represent the energy-dispersive x-ray (EDX) spectra of the TiO_2 nanoparticles prepared with 40%, 60%, and 100% of microwave power. The EDX analysis confirmed the atomic composition of the prepared samples. The results show that the spectra consist of titanium (Ti) and oxygen (O) peaks with high intensity, which represents the successful synthesis of highly-pure TiO_2 nanoparticles. The other weak peaks were attributed to impurities during the sample preparation for EDX analysis, such as silicon (Si).

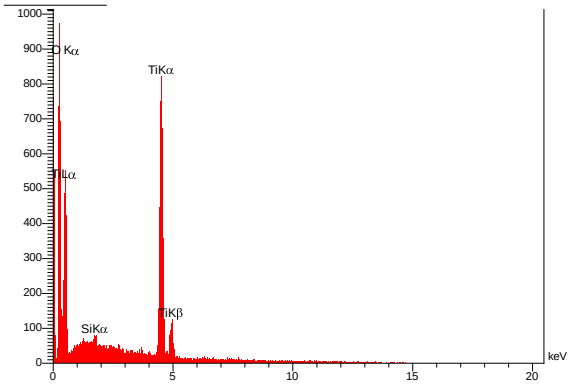

Fig. (12) EDX spectrum of TiO_2 nanoparticles synthesized with 40% microwave power

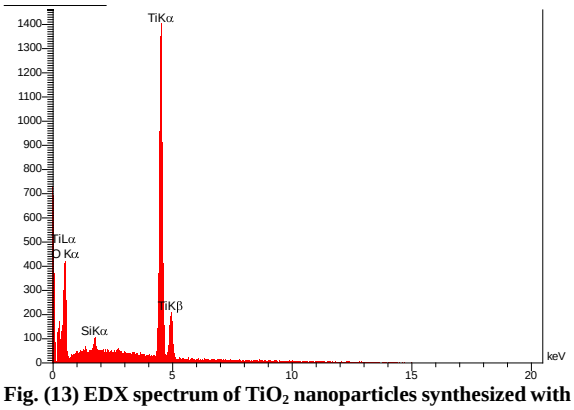

Fig. (13) EDX spectrum of TiO_2 nanoparticles synthesized with 60% microwave power

Figure (15) shows the Fourier-transform infrared (FTIR) spectrum of the prepared TiO_2 nanoparticles and its bond positions are summarized in table (3). The absorption band below 950 cm^{-1} is distinguishing vibrations of the inorganic Ti-O-Ti stretching in TiO_2 molecule. The peak at 733.32cm^{-1} was assigned to Ti-O-Ti stretching vibrations in the anatase phase, which signified that the strong absorbance of TiO_2 due to Ti-

O stretching turned into Ti-O-Ti bridge stretching or bending vibrations [19].

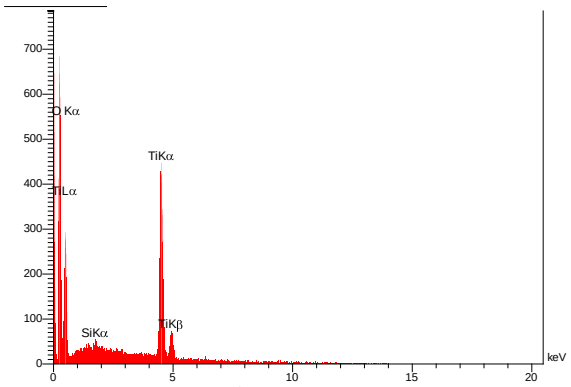

Fig. (14) EDX spectrum of TiO_2 nanoparticles synthesized with 100% microwave power

The broad absorption band at 3300-3800 cm^{-1} was ascribed to the stretching vibration of the hydroxyl O-H group at 3422-3789 cm^{-1}, which is due to the physical absorption of water and indicates the presence of moisture in the samples [20,21]. The peak at 2916 cm^{-1} can be attributed to the asymmetric stretching of the CH_3 terminal groups of the alkyl chain [22]. The weak bands at 1623 and 1111 cm^{-1} are assigned to O-H bending groups due to the chemically absorbed water in the solution [20].

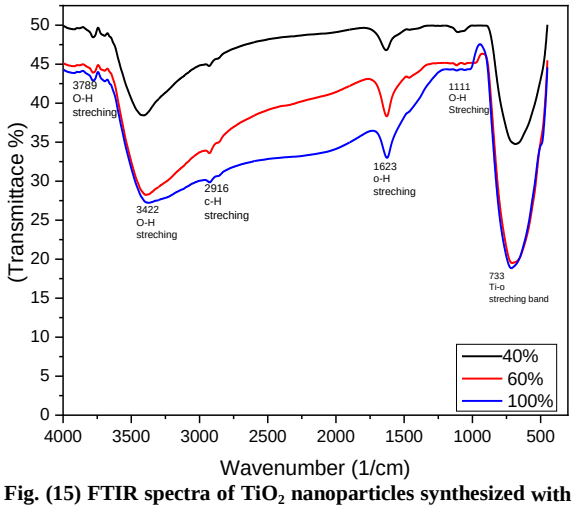

Fig. (15) FTIR spectra of TiO_2 nanoparticles synthesized with different microwave powers

Table (3) The vibrational bonds of the synthesized TiO_2 samples according to FTIR spectrum

Assignments	Wavenumbers (cm^{-1})
O – H stretching	3798
O – H stretching	3422
C – H stretching	2916
O – H bending	1623
C = O stretching	1111
Ti-O-Ti stretching	733

4. Conclusion

The results suggest that the utilization of microwave radiation offers a direct, efficient, and convenient method for the synthesis of titanium dioxide nanoparticles. The utilization of microwave-induced heating presents several potential benefits compared to conventional heating techniques, as it can facilitate or enhance chemical reactions. The synthesized TiO_2 nanoparticles exhibited a high degree of crystallinity and were in the anatase phase. The surface area of the prepared nanoparticles was within the range of 72.727-108.28 m^2/g. The TiO_2 samples showed average particle size ranging from 52.707 to 82.095 nm. Highly-pure TiO_2 nanoparticles were successfully produced.

References

[1] C.L. Pang, R. Lindsay and G. Thornton, "Chemical reactions on rutile TiO_2 (110)", *Chem. Soc. Rev.*, 37(10) (2008) 2328-2353.
[2] F.J. Al-Maliki, O.A. Hammadi and E.A. Al-Oubidy, "Optimization of Rutile/Anatase Ratio in Titanium Dioxide Nanostructures prepared by DC Magnetron Sputtering Technique", *Iraqi J. Sci.*, 60(special issue) (2019) 91-98.
[3] O.A. Hammadi, "Effects of Extraction Parameters on Particle Size of Titanium Dioxide Nanopowders Prepared by Physical Vapor Deposition Technique", *Plasmonics*, 15(6) (2020) 1747-1754.
[4] Z.H. Zaidan, Q.H. Mahmood and O.A. Hammadi, "Using Banana Peels for Green Synthesis of Mixed-Phase Titanium Dioxide Nanopowders", *Iraqi J. Appl. Phys.*, 18(4) (2022) 27-30.
[5] Z.H. Zaidan, O.A. Hammadi and K.H. Mahmood, "Effect of Structural Phase on Photocatalytic Activity of Titanium Dioxide Nanoparticles", *Iraqi J. Appl. Phys.*, 19(3A) (2023) 55-58.
[6] A. Kumar, "Different methods used for the synthesis of TiO_2 based nanomaterials: A review", *Am. J. Nano. Res. Appl.*, 38(1) (2018) 2243-2531.
[7] B. Ding et al., "Titanium dioxide nanofibers prepared by using electrospinning method", *Fibers Polymers*, 5(6) (2004) 105-109.
[8] O.A. Hammadi, F.J. Kadhim and E.A. Al-Oubidy, "Photocatalytic Activity of Nitrogen-Doped Titanium Dioxide Nanostructures Synthesized by DC Reactive Magnetron Sputtering Technique", *Nonl. Opt. Quantum Opt.*, 51(1-2) (2019) 67-78.
[9] F.J. Al-Maliki et al., "Enhanced photocatalytic activity of Ag-doped TiO_2 nanoparticles synthesized by DC Reactive Magnetron Co-Sputtering Technique", *Opt. Quantum Electron.*, 52 (2020) 188.
[10] F.J. Kadhim, O.A. Hammadi and N.H. Mutesher, "Photocatalytic activity of TiO_2/SiO_2 nanocomposites synthesized by reactive magnetron sputtering technique", *J. Nanophot.*, 16(2) (2022) 026005.
[11] J.G. Cuadra et al., "Multifunctional silver-coated transparent TiO_2 thin films for photocatalytic and antimicrobial applications", *Appl. Surf. Sci.*, 617 (2023) 156519.
[12] A.S. Barnard, P. Zapol and L.A. Curtiss, "Modeling the morphology and phase stability of

TiO_2 nanocrystals in water", *J. Chem. Theory Comput.*, 11(1) (2005) 107-116.
[13] D.K. Muthee and B.F. Dejene, "The effect of tetra isopropyl orthotitanate (TIP) concentration on structural, and luminescence properties of titanium dioxide nanoparticles prepared by sol-gel method", *Mater. Sci. Semicond. Process.*, 106 (2020) 104783.
[14] C. Liu, "A study of particle generation during laser ablation with applications", PhD diss., University of California, Berkeley (USA) (2005).
[15] G.M. AI-Rumahi, "Fabrication and Characterization of TiO_2 Dye Sensitized Solar Cells", J. Kufa Phys., 13(1) (2021) 43-48.
[16] K.L. Cao et al., "Sustainable porous hollow carbon spheres with high specific surface area derived from Kraft lignin", *Adv. Powder Technol.*, 32(6) (2021) 2064-2073.
[17] A.M. Negrescu et al., "Metal Oxide Nanoparticles: Review of Synthesis, Characterization and Biological Effects", *J. Funct. Biomater.*, 13(4) (2022) 274.
[18] A. Hindy et al., "Synthesis and characterization of 3D-printed functionally graded porous titanium alloy", *J. Mater. Sci.*, 55 (2020) 9082-9094.
[19] A.J. Moreira et al., "Photoactivity of boron-or nitrogen-modified TiO_2 for organic pollutants degradation: Unveiling the photocatalytic mechanisms and by-products", *J. Enviro. Chem. Eng.*, 11(1) (2023) 109207.
[20] S.L. Brantley and N.P. Mellott, "Surface area and porosity of primary silicate minerals", *Am. Mineralogist*, 85(11-12) (2000) 1767-1783.
[21] S.A. Hasan, J.A. Salman and S.S. Al-Jubori, "Characterization of Titanium Dioxide (TiO_2) Nanoparticles Biosynthesized using *Leuconostoc spp.* Isolated from Cow's Raw Milk: Characterization of TiO_2 Nanoparticles", *Proc. Pakistan Acad. Sci.: B. Life Enviro. Sci.*, 60(1) (2023) 133-142.
[22] M. Fathy and H. Hamad, "Influence of calcination temperatures on the formation of anatase TiO_2 nanorods with a polyol-mediated solvothermal method", *RSC Adv.*, 6(9) (2016) 7310-7316.

